Deformed odd-odd ^{180,182,184}Re isotopes in the interacting-boson model

W.-T. Chou and Wm. C. McHarris
National Superconducting Cyclotron Laboratory and Departments of Chemistry and of Physics and Astronomy, Michigan State University, East Lansing, Michigan 48824

Olaf Scholten
Kernfysisch Versneller Instituut, 9747 AA Groningen, The Netherlands
(Received 31 August 1987)

We present the detailed results of calculations of excitation-energy spectra, quadrupole and magnetic moments, and $B(E2)$ and $B(M1)$ values for the odd-odd ^{180,182,184}Re isotopes in the framework of the interacting-boson-fermion-fermion approximation model. Also, calculations are presented for both positive- and negative-parity excitations in the nearby odd-mass Re and Os nuclides and for collective states in the even-even Os core nuclides. The calculated results are compared with experimental data.

I. INTRODUCTION

The interacting-boson approximation (IBA) model[1-7] has proven to be able to give a rather accurate description of the properties of low-lying collective states in even-even nuclei. Likewise, its extension to odd-mass nuclei, the interacting-boson-fermion approximation (IBFA) model,[8-10] is able to reproduce a large variety of properties in phenomenological calculations. In this paper we examine the extension of the model to odd-odd nuclei, where we call it the interacting-boson-fermion-fermion approximation (IBFFA) model.

Odd-odd nuclei have been calculated before in the framework of the IBA model. The earliest calculations were done using supersymmetries[11,12] and were applied to nuclei in the Pt-Au region. With the use of these symmetries it becomes possible to treat rather complicated systems in a very simple manner. This has made it possible to perform many of these calculations even without the use of large computers. The disadvantage of such methods is that they assume the Hamiltonian of the system exhibits specific symmetries. In realistic cases such symmetries are present in only relatively few nuclei. The large majority of nuclei do not lend themselves to such treatment; hence, a full numerical treatment has to be done. Paar *et al.*[13] and Blasi *et al.*[14] have performed calculations of this sort. However, in order to keep the calculations tractable, they had to limit themselves to only the unique-parity orbits. Similarly, calculations of two-quasiparticle states in even-even nuclei[15-19] within the IBA framework have been limited to unique-parity orbits. In our present work we present calculations for odd-odd nuclei where there is no restriction to unique-parity orbits. These calculations were made possible by the particular, very efficient model-space truncation scheme used.

We selected the present odd-odd isotopes of $_{75}$Re because of the long-standing interest in these nuclides by some of us,[20,21] and because reasonably well-understood experimental data exist for all three odd-odd isotopes in a series[20,22-24] and for many nearby odd-mass nuclides. In addition, the even-even Os cores of these nuclei are well deformed, which makes it possible to compare the IBA model predictions with those of the geometrical Bohr-Mottelson model.[25]

In Sec. II we present a short outline of the IBA model and its applications to the even-even Os isotopes. These will serve as the cores to which the odd particles are coupled in the subsequent calculations for the odd-mass nuclides and odd-odd Re isotopes. In Sec. III we discuss the case of the coupling of a single odd particle to the core, the IBFA model. There we present our results for the odd-mass Re and Os isotopes. These calculations serve to determine the parameters that govern the coupling of the odd proton and odd neutron to the even-even Os cores. In Sec. IV we cover the actual calculations for the three odd-odd Re isotopes, including an outline of the IBFFA model used and some details of the calculations. Finally, in Sec. V we summarize our results and make qualitative comparisons both with experimental data and with the predictions that follow from the Bohr-Mottelson model.

II. THE EVEN-EVEN ^{182,184,186}Os CORES

A. Excitation energies

To describe the structure of an odd-mass or an odd-odd nucleus in the IBA model, first a description of the appropriate even-even core should be obtained. Since in the $^{A}_{75}$Re nuclei the protons are past the middle of the 82–126 major shell, the $^{A+2}_{76}$Os nuclei constitute the even-even cores. The bosons are holelike, and therefore only the degrees of freedom of a hole should be coupled to the system of bosons.

In the odd-odd nuclei we will be interested exclusively in states below 2 MeV in excitation energy. Only the structures of the lowest-lying states in the even-even core will enter into the calculations for these odd-odd states. Since these are predominantly symmetric in the proton-

neutron degree of freedom, a description in terms of the IBA-1 model,[26] where no explicit distinction is made between proton and neutron excitations, is sufficient. A simplified IBA-1 Hamiltonian is used,

$$H=n_d\epsilon_d+\kappa' L\cdot L+\kappa Q\cdot Q \ . \tag{1}$$

Here n_d is the number of d-wave bosons at an energy ϵ_d, $L\cdot L$ is the "dipole" or angular-momentum interaction, and $Q\cdot Q$ is the quadrupole interaction. Specifically,

$$L=\sqrt{10}(d^{\dagger}\tilde{d})^{(1)} \tag{2}$$

and

$$Q=(s^{\dagger}\tilde{d}+d^{\dagger}s)^{(2)}+\chi(d^{\dagger}\tilde{d})^{(2)} \ . \tag{3}$$

The constants κ, κ', and χ are determined empirically. The set of parameters we used for our calculations, adjusted so as to obtain the best overall agreement in the excitation-energy spectra, are listed in Table I.

(It should be noted that our parameters in Table I differ slightly from those in Ref. 6, where calculations were performed for $^{188-196}$Pt and $^{186-194}$Os. The Hamiltonian in general can be written as

$$H=n_d\epsilon_d+\kappa'' P\cdot P+\kappa' L\cdot L+\kappa Q\cdot Q \ . \tag{1a}$$

For our calculations we used the simplified Hamiltonian [Eq. (1)] for the SU(3) limit, which corresponds to $\kappa'=0$. The calculations of Ref. 6 dealt with somewhat higher-mass numbers, close to the O(6) limit, which corresponds to $\kappa=0$. Thus, they performed calculations in a perturbed O(6) scheme by introducing a finite $Q\cdot Q$ interaction, whose strength increases with increasing distance from ^{196}Pt).

The calculated energies are compared with experimental energies[27–29] in Fig. 1. All three isotopes show a well-developed ground-state rotational band, while some staggering is observed in the γ-vibrational bands. Our calculations reproduce this, although they overestimate the staggering in the γ-vibrational bands. No other collective excitations, such as β-vibrational bands, have been observed in these nuclei. In our calculations the β-vibrational bands lie above 1.1 MeV in excitation.

TABLE I. IBA parameters for the even-even Os core nuclei.

A	182	184	186
N	106	108	110
ϵ_d (MeV)	0.500	0.470	0.440
κ' (MeV)	0.0000	0.0005	0.0015
κ (MeV)	−0.0200	−0.0235	−0.0245
χ (dimensionless)	−0.537	−0.581	−0.514
χ_T (dimensionless)	−0.236	−0.212	−0.195
e_B (e b)	0.142	0.144	0.147

B. Electromagnetic properties

Since at a later stage we shall calculate electromagnetic properties for the odd-odd nuclei, we need to determine the boson effective charge and the d-boson g factor by reproducing the relevant quantities in the even-even core nuclei.

The operator used in the calculation of quadrupole properties is

$$T^{(E2)}=e_B[(s^{\dagger}\tilde{d}+d^{\dagger}s)^{(2)}+\chi_T(d^{\dagger}\tilde{d})^{(2)}] \ , \tag{4}$$

where e_B is the boson effective charge. In the $E2$ operator the boson effective charge and the parameter χ_T were adjusted so as to obtain the best overall agreement with the experimental $B(E2)$ values.

Some calculated and experimental[30,31] $B(E2)$ values for important transitions in the even-even Os isotopes are shown in Fig. 2, and electric quadrupole moments are

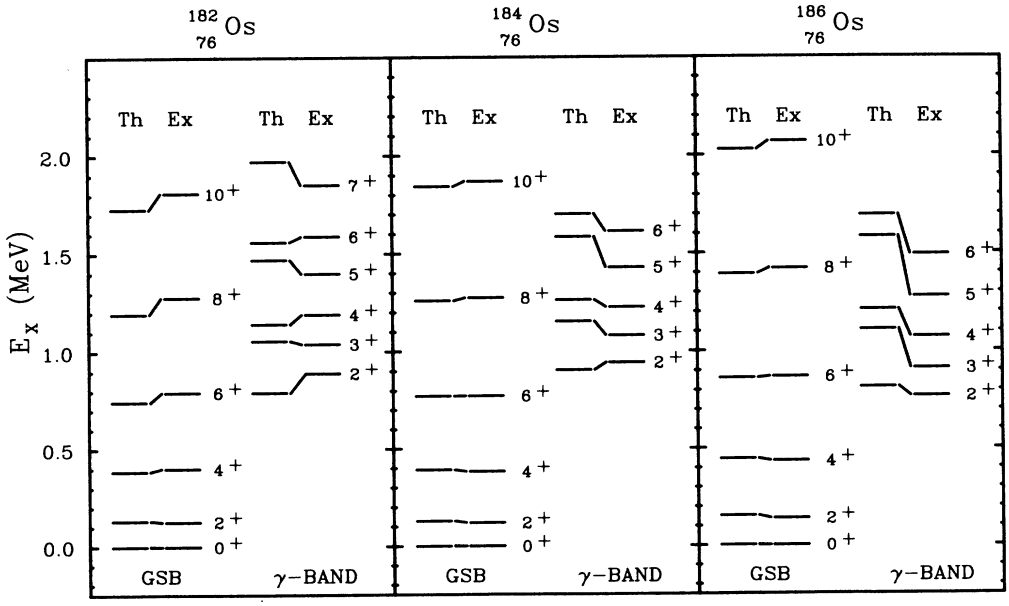

FIG. 1. IBA-calculated excitation-energy spectra for the even-even Os core isotopes compared with experimental data.

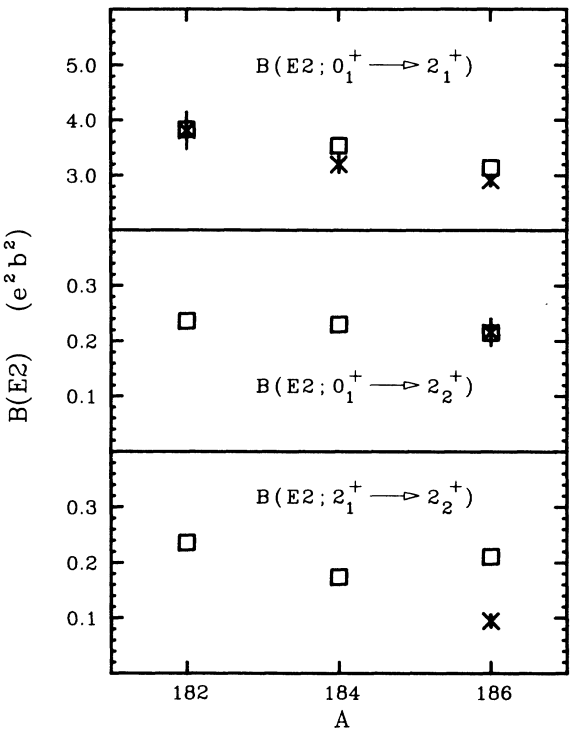

FIG. 2. IBA-calculated $B(E2)$ values for the even-even Os core isotopes compared with experimental values. The squares are the calculated values; the $\times$'s (with error bars), the experimental values.

shown in Fig. 3. We used the experimental $B(E2)$ values for the $0_1^+ \rightarrow 2_1^+$ and $0_1^+ \rightarrow 2_2^+$ transitions (the $2_1^+ \rightarrow 2_2^+$ transition was not used because of the possibility of $M1$ admixture; note that the agreement is less good for this transition) and varied the values for e_B and χ_T in order to get the best fit. [It has been checked for ^{186}Os that other known $B(E2)$ values are also reproduced.]

The $M1$ operator can be written as

$$T^{(M1)}=g_d\sqrt{10}(d^\dagger\tilde{d})^{(1)} , \tag{5}$$

where g_d is the d-boson g factor. By comparing Eq. (5) with Eq. (2), it can be seen that the $M1$ operator is proportional to the total angular-momentum operator L in the boson space. This operator thus does not induce $M1$ transitions but only magnetic moments. For even-even medium-heavy nuclei, this is realistic, since $B(M1)$ values are indeed very small compared with the magnetic moments. From the value of the known g factors of the 2_1^+ states we deduce that $g_d=0.25\ \mu_N$ for the d-boson g factor.[32]

III. THE ODD-MASS NUCLEI

A. Short discussion of theory

Odd-mass nuclei are described in the framework of the IBA model by coupling the degrees of freedom of a single odd particle to the system of s and d bosons that describes the even-even core nucleus. The general Hamiltonian for such a system can be written as

$$H_{\rm IBFA}=H_{\rm IBA}+H_F+V_{\rm BF} , \tag{6}$$

where $H_{\rm IBA}$ is the usual s-d boson Hamiltonian as given by Eq. (1), H_F is the fermion Hamiltonian, and $V_{\rm BF}$ is the boson-fermion coupling interaction. Since only a single odd particle is coupled to the bosons, H_F contains only one-body terms:

$$H_F=\sum_{jm}\epsilon_j a_{jm}^\dagger a_{jm} , \tag{7}$$

where $a_{jm}^\dagger$ (or a_{jm}) is the creation (or annihilation) operator for an odd particle in the state $|jm\rangle$ and ϵ_j are the single quasiparticle energies. Most of the interesting physics goes into the structure of the boson-fermion interaction:

$$V_{BF}=\sum_{jj'}\Gamma_{jj'}(Q^{(2)}\cdot(a_j^\dagger\times\tilde{a}_{j'})^{(2)})+\sum_{jj'j''}\Lambda_{jj'}^{j''}:[(d^\dagger\times\tilde{a}_j)^{(j'')}\times(a_{j'}^\dagger\times\tilde{d})^{(j'')}]_0^{(0)}:+\sum A_0 N_d\cdot N_j , \tag{8}$$

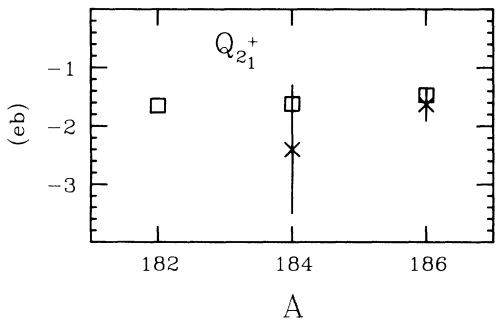

FIG. 3. IBA-calculated Q values for the 2_1^+ state in the even-even Os core isotopes compared with experimental values. The squares are the calculated values; the $\times$'s, the experimental values.

where

$$Q^{(2)}=(s^\dagger\times\tilde{d}+d^\dagger\times s)^{(2)}+\chi(d^\dagger\times\tilde{d})^{(2)} , \tag{9}$$

$$\tilde{d}_m=(-1)^m d_m , \tag{10}$$

and

$$\tilde{a}_{jm}=(-1)^{j-m}a_{j-m} . \tag{11}$$

The first term in Eq. (8) represents the direct component of the quadrupole interaction between the odd particle and the bosons. Because of the two-particle nature of the bosons, bringing the Pauli exclusion principle into play, there is also an exchange component, which is represented by the second term. The last term, the monopole force, can result from a variety of causes, in particular

from the blocking of certain degrees of freedom by the odd particle. In practical calculations the strength of the third term is such that it has only a minor influence on the structure of the spectrum.

On the basis of a microscopic model[26,33] one can estimate the dependence of the coupling coefficients $\Gamma_{jj'}$ and $\Lambda^{j''}_{jj'}$ on the spins as

$$\Gamma_{jj'}=\Gamma_0(u_j u_{j'}-v_j v_{j'})Q_{jj'} \tag{12}$$

and

$$\Lambda^{j''}_{jj'}=-2\sqrt{5}\Lambda_0\beta_{jj''}\beta_{j''j'}/(2j''+1)^{1/2}\ , \tag{13}$$

with

$$\beta_{jj'}=\langle j\|Y^{(2)}\|j'\rangle(u_j v_{j'}+v_j u_{j'}) \tag{14}$$

and

$$u_j^2=1-v_j^2\ . \tag{15}$$

The coefficients v_j are related to the structure coefficients of the fermion S-pair state, which is the microscopic equivalent of the s boson in the IBA model. In practice, these are taken equal to the occupation probabilities of the single-particle orbits, as follows from a spherical BCS calculation. The effects from deformation are taken into account in the IBFA calculation. The coefficients $\beta_{jj'}$ are the structure coefficients of the d bosons. A first-order guess for their values is given by Eq. (14).

B. ^{181,183,185}Re: odd-proton couplings

1. Excitation energies

The $_{75}$Re isotopes are described in the IBFA model by coupling the degrees of freedom of a single-proton hole to an $_{76}$Os core. The calculations were performed separately for positive- and negative-parity states. In the description of negative-parity states, in addition to the $h_{11/2}$ unique-parity orbit in the $Z=50-82$ shell, we also included the $h_{9/2}$ orbit from the next major shell because states originating from it have been observed experimentally. Since we included the $h_{9/2}$ state in the basis set, for consistency we included all positive-parity orbits ($g_{7/2}$, $d_{5/2}$, $d_{3/2}$, and $s_{1/2}$) from $Z=50-82$ shell, even though the last two have rather high single-particle energies.

In the calculation of negative-parity states, all parameters describing the boson-fermion interaction, including occupation probabilities, were adjusted so as to yield a best agreement with the experimental excitation energies. The only constraint on the parameters was that they vary smoothly and systematically from isotope to isotope. The same principle was followed for calculating positive-parity states, except that the occupation probabilities were calculated via the BCS formalism. The single-particle energies used in the BCS calculations are listed in Table II. These values were extrapolated from the experimental single-particle energies of nuclei having closed-shell configurations. To improve the fit, in some instances they were varied by no more than 200 keV. The complete sets of parameters used in the calculations are listed for negative-parity states in Table III and for positive-parity states in Table IV. Note that the occupation probabilities are such that all particles in the $Z=50-82$ valence shell are accounted for.

TABLE II. Single-particle energies for odd-mass Re positive-parity states.

	$g_{7/2}$	$d_{5/2}$	$d_{3/2}$	$s_{1/2}$
^{181}Re	0.000 MeV	1.285	2.509	2.491
^{183}Re	0.000	1.202	2.522	2.489
^{185}Re	0.000	1.125	2.555	2.487

The Re isotopes lie in the well-deformed region, and their excitation-energy spectra clearly show features of rotational bands. All three isotopes in which we are interested have similar spectra: $K^\pi=5/2^+$ for the ground-state rotational band and $9/2^-$ for the second lowest-lying band. Another band, having $K^\pi=1/2^-$ and originating from the spherical $h_{9/2}$ state, lies fairly low in ^{181}Re, but its energy increases with increasing mass number, and its position is unclear in ^{185}Re. A point to note is that the spacing between the $5/2^-$ and $9/2^-$ members of the $K^\pi=1/2^-$ band is uncertain because the transition energy is too low for the γ-ray to have been observed. In Ref. 34 the given systematics for these energies were determined from coriolis-coupling calculations and systematics.

We show a comparison between calculated and experimental[34–38] excitation energies for the negative-parity states in Fig. 4. The $K^\pi=9/2^-$ rotational band has a large $h_{11/2}$ single-particle component, the only negative-parity orbit in the $Z=50-82$ shell. The other band, $1/2^-$, has a large $h_{9/2}$ component coming from the next major shell. (Although this band is not too well defined in ^{185}Re, we show it for consistency.) Our calculations reproduce the rotational features of these two bands quite well, including the strong decoupling in the $1/2^-$ band. Members of the signature $=+1/2$ branch of this band were fit somewhat better than members of the $-1/2$ branch. It may be necessary to include more single-particle orbits from the next major shell, e.g., $f_{7/2}$, in order to improve the fits to this $1/2^-$ band. However, this would make the calculation considerably more complicated, which we wanted to avoid. It should be noted that in our calculations we did not employ a coriolis-force attenuation. Had we included this as a free parameter, as is often done in calculations for odd-mass nuclei, we would

TABLE III. IBFA parameters for odd-mass Re negative-parity states.

	^{181}Re	^{183}Re	^{185}Re
Λ_0^-	1.40	1.48	1.68
Γ_0^-	0.736	0.627	0.510
A_0^-	−0.10	−0.10	−0.10
χ	−1.20	−1.20	−1.20
$v^2h_{11/2}$	0.62	0.65	0.68
$v^2h_{9/2}$	0.05	0.05	0.05
E (MeV) $h_{9/2}$	3.125	2.350	2.036

TABLE IV. IBFA parameters for odd-mass Re positive-parity states.

	^{181}Re	^{183}Re	^{185}Re
Λ_0^+	0.730	0.875	1.013
Γ_0^+	0.496	0.380	0.363
A_0^+	0.00	−0.10	−0.10
χ	−1.20	−1.20	−1.20
$v^2g_{7/2}$	0.970	0.968	0.966
$v^2d_{5/2}$	0.914	0.913	0.912
$v^2d_{3/2}$	0.623	0.574	0.512
$v^2s_{1/2}$	0.631	0.590	0.545

certainly have been able to improve our fits.

Results for the positive-parity states are shown in Fig. 5. Fits are very good for the $5/2^+$ ground-state rotational bands and reasonable for the other hands. The excitation energies for the band heads could probably be improved by varying the single-particle energies in the calculations. But we chose not to do that as long as an overall reasonable fit could be achieved. Other positive-parity bands in these three Re isotopes either have higher excitation energies or are not well known experimentally, so we do not consider them further in this investigation.

2. *B(E2) values and quadrupole moments*

In the IBFA model the $E2$ transition operator contains contributions both from the bosons and from the odd fermion:

$$T^{(E2)}=e_B Q_B+e_F Q_F \ . \tag{16}$$

Here Q_B is the same as Q defined in Eq. (4), while

$$Q_F=\sum_{jj'} Q_{jj'}(a_j^\dagger \tilde{a}_{j'})^{(2)} \ . \tag{17}$$

(For simplicity we have omitted a possible exchange term in Q_F.[26]) We used the e_B values given in Sec. II B for the Os cores; also $e_F=e_B$.[10]

Some selected $B(E2)$ values for crossover and stopover transitions between lower-lying members of the more well-defined bands are shown in Fig. 6. The contributions from the odd fermion appear to be rather small for these transitions, as can be seen from the fact that the curve for the three isotopes can almost be superimposed. (This is not always true, as will be noted for the odd-mass Os isotopes in Sec. III C 2.) The quadrupole moments of some low-lying band heads are shown in Fig. 7. Unfortunately, the experimental data are relatively few,[39–43] making it difficult to obtain quantitative tests of the values. However, data do exist[43] for the

$$5/2^+7/2[402\uparrow]\rightarrow 5/2^+5/2[402\uparrow]$$

and

$$5/2^+9/2[402\uparrow]\rightarrow 5/2^+5/2[402\uparrow]$$

transitions in ^{185}Re. The respective experimental (calculated) $B(E2)$ values are 1.0 (1.24) and 0.31 (0.36) e b.

3. *Magnetic moments and B(M1) values*

Contrary to the case of the electric quadrupole properties, the magnetic properties of odd-mass nuclei depend strongly on the properties of the odd particle, so they should provide a good test of the wave functions. For our $M1$ operator we used

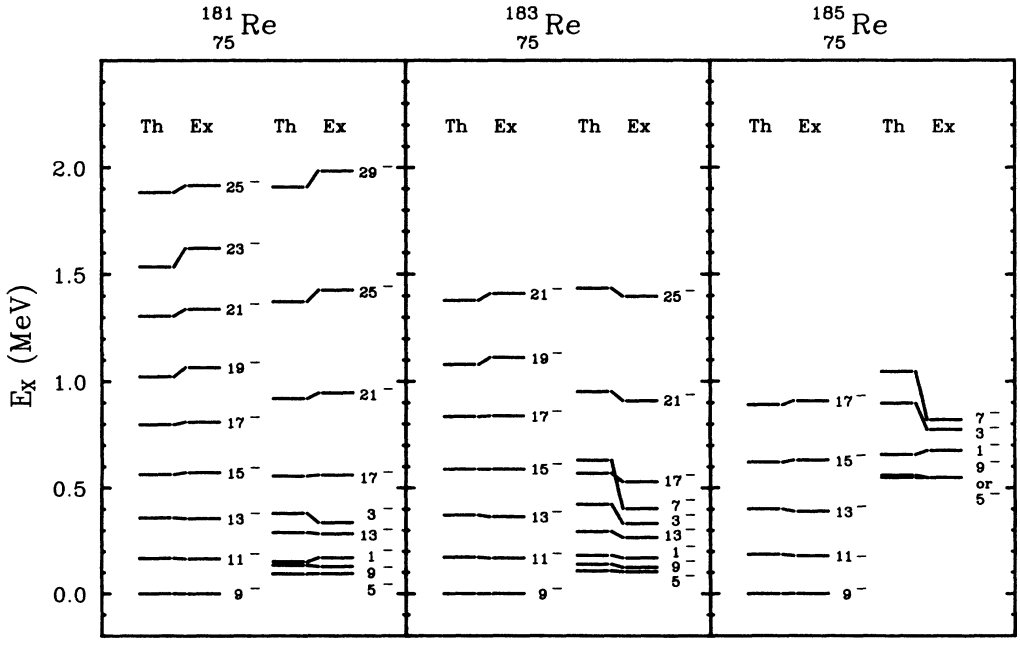

FIG. 4. IBFA-calculated excitation energies for negative-parity states in the odd-mass Re isotopes compared with experimental data. States are labeled with $2J$.

$$T^{(M1)}=\sqrt{3/4\pi}\left[g_d\sqrt{10}(d^\dagger\tilde{d})^{(1)}-\sum_{jj'}g_{jj'}\sqrt{j(j+1)(2j+1)/3}(a_j^\dagger\tilde{a}_{j'})^{(1)}\right], \tag{18}$$

where

$$\begin{aligned} g_{jj'}&=[(2j-1)g_l+g_s]/2j \quad \text{for } j=l+\tfrac{1}{2}=j' ,\\ g_{jj'}&=[(2j+3)g_l-g_s]/2(j+1) \quad \text{for } j=l-\tfrac{1}{2}=j' ,\\ g_{jj'}&=(g_l-g_s)\sqrt{2l(l+1)/j(j+1)(2j+1)(2l+1)} \\ &\qquad \text{for } j'=l-\tfrac{1}{2}=j-1, \quad l'=l . \end{aligned} \tag{19}$$

We extracted the boson g factor from the magnetic moment of the 2_1^+ states in the even-even Os cores,[32] obtaining a value of $g_d=0.25$ nm. Following the procedure used for similar calculations in the Eu isotopes,[10] we quenched the value of g_s by a factor of 0.7 from the single-particle estimate down to 4.0 nm.

Some selected magnetic moments are shown in Fig. 8. It can be seen that they are determined essentially by the fermion part of the operator, Eq. (18). Some calculated $B(M1)$ values are shown in Fig. 9. Unfortunately, no experimental data exist at this time to test the predictions.

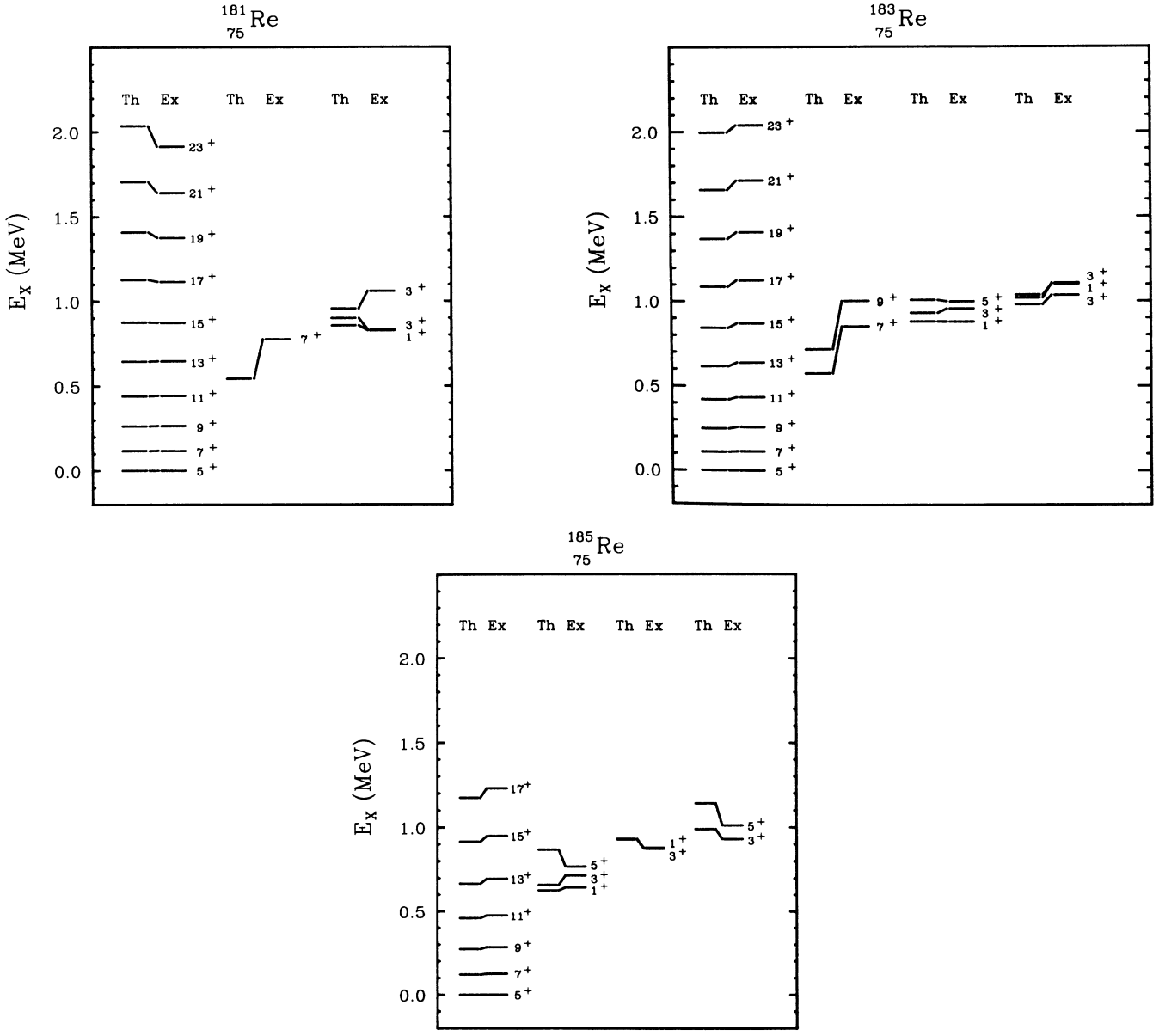

FIG. 5. IBFA-calculated excitation energies for positive-parity states in the odd-mass Re isotopes compared with experimental data. States are labeled with $2J$.

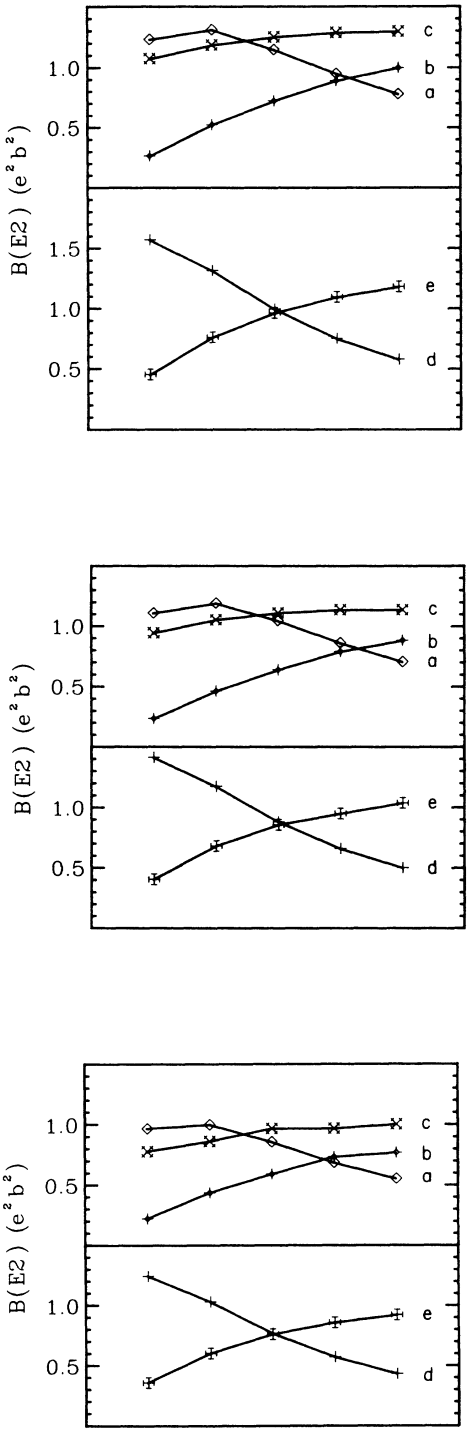

FIG. 6. IBFA-calculated $B(E2)$ values for selected crossover and stopover transitions in low-lying bands in the odd-mass Re isotopes. Top, the values for ^{181}Re; middle, for ^{183}Re; and bottom, for ^{185}Re. Within each figure the curves represent transitions in bands as follows: a, $9/2^-$ stopover; b, $9/2^-$ crossover; c, $1/2^-$ crossover; d, $5/2^+$ stopover; e, $5/2^+$ crossover. The left-most point represents the lowest transition of its kind in that band, with the successively higher transitions following in order. Thus, in $9/2^-$ crossover set (curve b), the transitions would be, from left to right, $13/2^- \rightarrow 9/2^-$, $15/2^- \rightarrow 11/2^-$, $17/2^- \rightarrow 13/2^-$, $19/2^- \rightarrow 15/2^-$, and $21/2^- \rightarrow 17/2^-$.

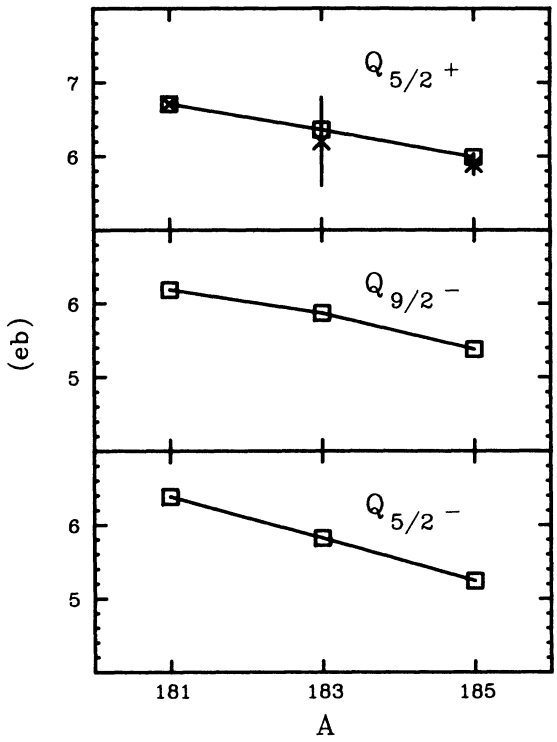

FIG. 7. IBFA-calculated Q values for selected band-head states in the odd-mass Re isotopes compared with a few experimental data. The squares are the calculated values; the $\times$'s, experimental values. (The $5/2^+$ point for ^{181}Re is an independently calculated rather than an experimental value.)

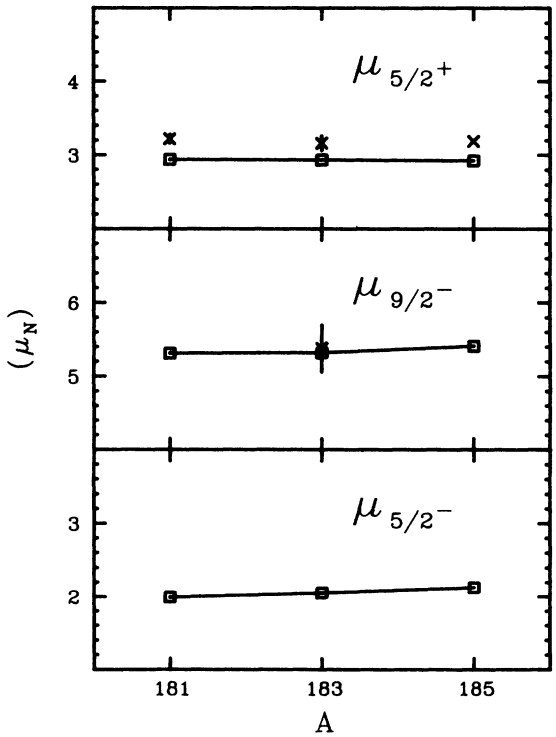

FIG. 8. IBFA-calculated μ values for selected band-head states in the odd-mass Re isotopes compared with a few experimental data. The squares are the calculated values; the $\times$'s, the experimental values.

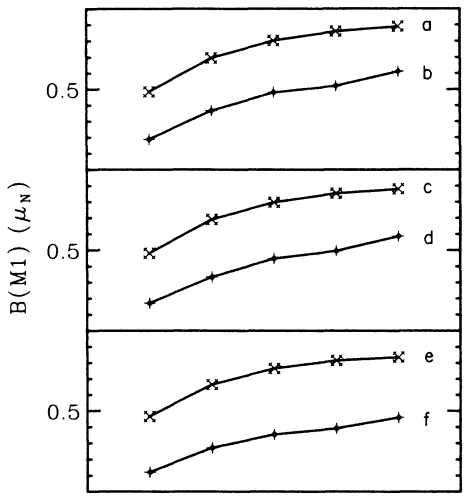

FIG. 9. IBFA-calculated $B(M1)$ values for selected transitions between low-lying rotational-band members in the odd-mass Re isotopes. The points correspond to the following bands. ^{181}Re: *a*, $9/2^-$ band. *b*, $5/2^+$ band. ^{183}Re: *c*, $9/2^-$; *d*, $5/2^+$. ^{185}Re: *e*, $9/2^-$; *f*, $5/2^+$. The transitions between lowest members of a band lie on the left, between higher members increasing systematically toward the right, as in Fig. 6.

C. ^{181,183,185}Os: odd-neutron couplings

1. Excitation energies

The odd-mass $_{76}$Os isotopes are described in the IBFA model by coupling the degrees of freedom of a single neutron hole to the appropriate even-even Os core. In general, the same procedure was followed as in the calculations for the odd-mass Re isotopes. Again, all the single-particle orbits in this region, the $N=82-126$ shell, were included. This made the calculations rather time consuming, so no detailed fit to the experimental excitation energies was attempted. The single-particle energies were obtained as in the Re case. For simplicity, we tried to keep these values constant; however, if no satisfactory results could be obtained with the initial values, they were modified (by no more than 300 keV) in order to obtain better agreement with experiment. The list of single-particle energies used is given in Table V. The complete sets of parameters used in the calculations are listed for positive-parity states in Table VI and for negative-parity states in Table VII.

For the odd-mass Os isotopes having $N=105$, 107, and 109, the $i_{13/2}$ orbit is the only positive-parity orbit entering the calculations. We show the results of the calculations for positive-parity states and compare them with experimental values[35–38,44–46] in Fig. 10.

As expected for high-j (low-Ω) orbits, coriolis coupling is strong for states originating from the $i_{13/2}$ state. Thus, there is a considerable amount of staggering for the positive-parity bands. Although the calculations do not show quite the same degree of staggering as has been observed experimentally, they do reproduce the features of these positive-parity bands reasonably well.

^{181}Os shows the greatest degree of staggering, and its $9/2^+$ band has been reported[35,36] as being a mixed $i_{13/2}$ band, namely the Nilsson states $9/2^+[624]$ and $7/2^+[633]$ combined; starting at $J=35/2$, states having signature $-1/2$ shift to higher energies with respect to states having signature $+1/2$. In our calculations we find the state with lowest energy to be $9/2$, with a $7/2$ state at 1.7 keV. This can very well explain the so-called mixed $i_{13/2}$ band. Our calculations also show states starting to reverse at spin $27/2$, although to a lesser degree than found in experiment.

Results for negative-parity states are compared with experiment in Fig. 11. Unfortunately, the negative-parity states in these odd-mass Os isotopes are not very well established.

For ^{181}Os and ^{183}Os a few low-energy members of signature $-1/2$ from a $K^\pi=1/2^-$ band have been reported from Ir decay[45,46] but have not been seen in reaction studies.[35,44] Thus, we expect that the staggering in the $K^\pi=1/2^-$ bands predicted in our calculations might be reasonable. The relative positions of the two band heads in ^{181}Os is not known experimentally. It was suggested[35] from systematics that the ground state is $7/2^-$, with the $1/2^-$ state lying at very low excitation energy. Because of this ambiguity, we did not try to force the $7/2^-$ to be

TABLE V. Single-particle energies for odd-mass Os negative-parity states.

	$f_{7/2}$	$h_{9/2}$	$p_{3/2}$	$f_{5/2}$	$p_{1/2}$
^{181}Os	0.000 MeV	0.460	1.700	1.880	2.220
^{183}Os	0.000	0.510	1.605	1.928	2.273
^{185}Os	0.000	0.560	1.505	1.978	2.323

TABLE VI. IBFA parameters for odd-mass Os positive-parity states.

	^{181}Os	^{183}Os	^{185}Os
Λ_0^+	2.820	2.021	2.010
Γ_0^+	0.486	0.468	0.307
A_0^+	−0.10	−0.10	−0.10
χ	−1.00	−1.00	−1.00
$v^2 i_{13/2}$	0.375	0.600	0.780

TABLE VII. IBFA parameters for odd-mass Os negative-parity isotopes.

	^{181}Os	^{183}Os	^{185}Os
Λ_0^-	0.732	0.800	1.100
Γ_0^-	0.286	0.190	0.120
A_0^-	−0.10	−0.10	−0.10
χ	−1.00	−1.00	−1.00
$v^2 f_{7/2}$	0.884	0.863	0.854
$v^2 h_{9/2}$	0.798	0.740	0.703
$v^2 p_{3/2}$	0.277	0.260	0.276
$v^2 f_{5/2}$	0.219	0.172	0.151
$v^2 p_{1/2}$	0.143	0.114	0.102

the ground state in our calculations but rather sought an overall good fit to these two close-lying bands. We obtained a $1/2^-$ ground state, with the $7/2^-$ band starting at 21.6 keV.

Spin assignments for the $7/2^-$ band in ^{185}Os are uncertain,[42] which made any precise determination of parameters for this nucleus rather difficult. We thus opted for a set of parameters that gave the best agreement with the experimental results for all three isotopes in a systematic way, under the assumption that the spin assignments were correct. This was done instead of forcing a best fit to individual sets of levels.

2. *Electromagnetic properties*

The electromagnetic properties of the odd-mass Os isotopes were calculated in the same manner as for the odd-mass Re isotopes, with the exception that $e_F=0$. There are not many experimental data available for comparison, so we had to rely more heavily here on systematics and what appear to be "reasonable" predictions. $B(E2)$ values for crossover and stopover transitions between lower-lying members of a few well-defined bands are shown in Fig. 12; Q_0 values for some low-lying band heads are shown in Fig. 13; selected values of μ are shown in Fig. 14; and some calculated $B(M1)$ values are shown in Fig. 15. Experimental data for the odd-mass Os isotopes are very scarce,[47,48] making meaningful comparisons difficult.

Interference effects are much more important for the Os isotopes than they were for the Re isotopes, particularly where $1/2^-$ states are involved. For example, compare the three curves for $B(M1)$ values in the $1/2^-$ band shown in Fig. 15—constructive and destructive interference effects are very apparent. Less immediately striking, but perhaps of more significance, are similar effects in the curves for $B(E2)$ values shown in Fig. 12. There the interference effects are sufficient to add appreciably to the normally-dominant core contributions—compare the values for ^{183}Os, in particular, with those for ^{181}Os and ^{185}Os. This presents a decided contrast to the very smooth behavior for the $B(E2)$ values for the Re isotopes shown in Fig. 6.

IV. THE ODD-ODD NUCLEI: ^{180}Re, ^{182}Re, AND ^{184}Re

A. Excitation energies

The Hamiltonian for deformed odd-odd nuclei can be written as follows:

$$H=H_{\mathrm{IBA}}+H_{\mathrm{p},F}+H_{\mathrm{n},F}+H_{\mathrm{p,BF}}+H_{\mathrm{n,BF}}+V_{\mathrm{pn}} \ . \qquad (20)$$

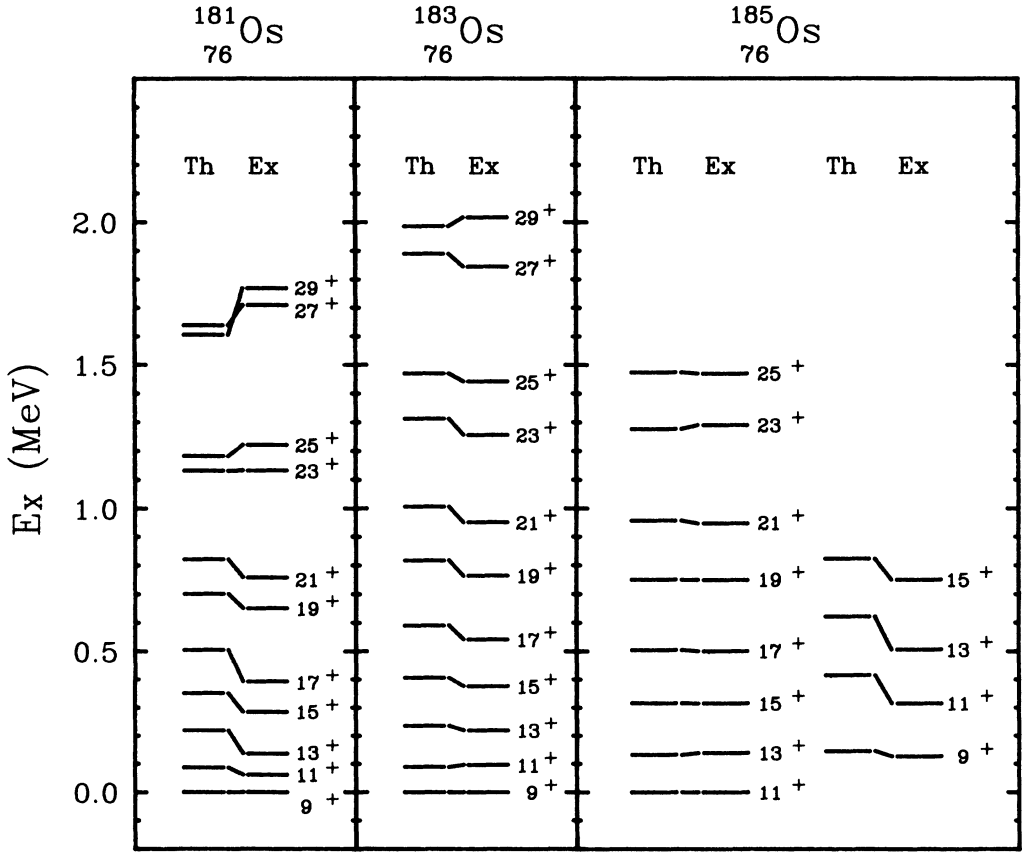

FIG. 10. IBFA-calculated excitation energies for positive-parity states in the odd-mass Os isotopes compared with experimental data. The states are labeled with $2J$.

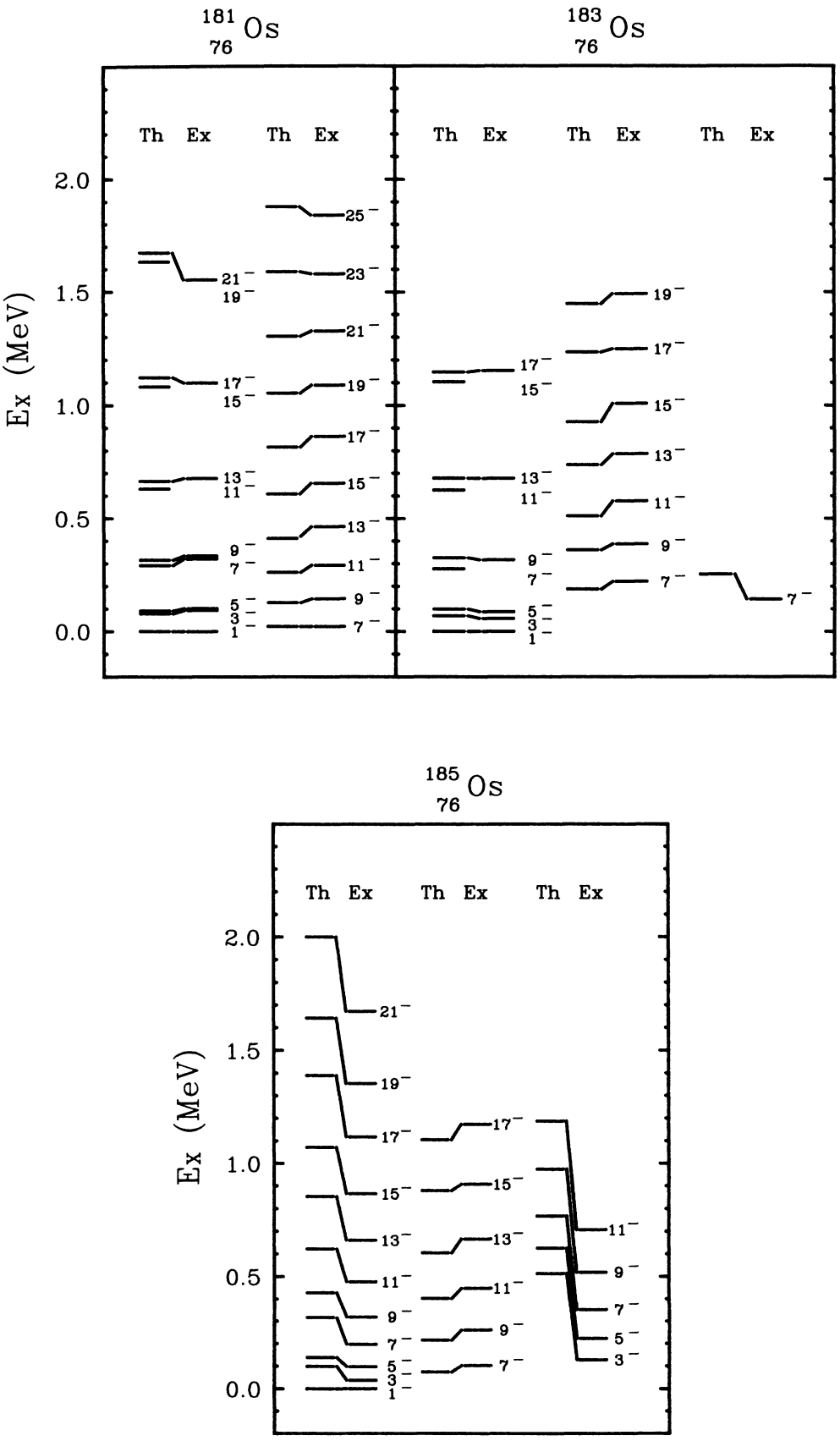

FIG. 11. IBFA-calculated excitation energies for negative-parity states in the odd-mass Os isotopes compared with experimental data. The states are labeled with $2J$.

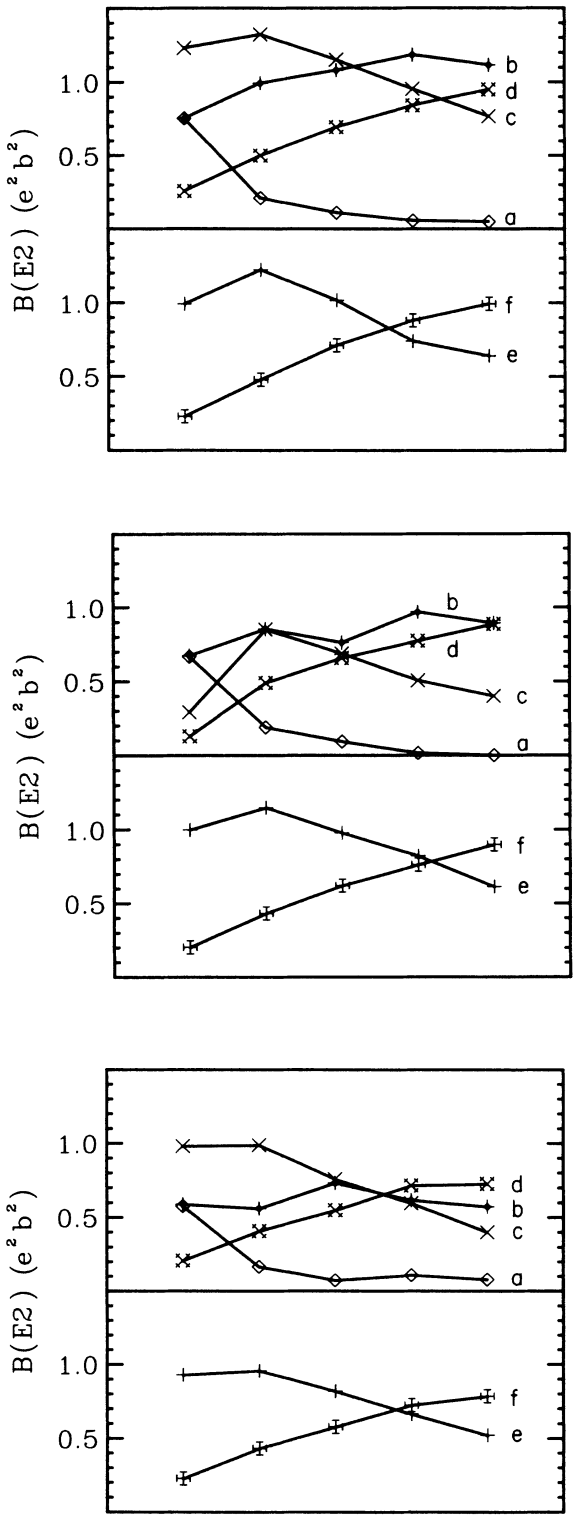

FIG. 12. IBFA-calculated $B(E2)$ values for selected crossover and stopover transitions in low-lying bands in the odd-mass Os isotopes. Top, the values for ^{181}Os; middle, for ^{183}Os; bottom, for ^{185}Os. Within each figure the curves represent transitions in bands as follows: *a*, $1/2^-$ band stopover; *b*, $1/2^-$ crossover; *c*, $7/2^-$ stopover; *d*, $7/2^-$ crossover; *e*, $9/2^+$ stopover; and *f*, $9/2^+$ crossover. The transitions between the lowest members of a band are on the left, between members increasing systematically toward the right, as in Fig. 6.

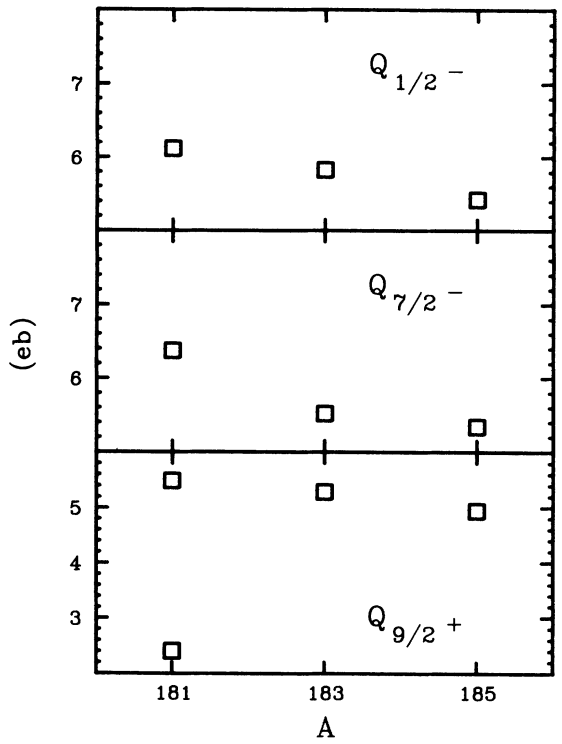

FIG. 13. IBFA-calculated Q values for selected band-head states in the odd-mass Os isotopes. (The extra lower point for ^{181}Os assumes a $7/2^+$ state.)

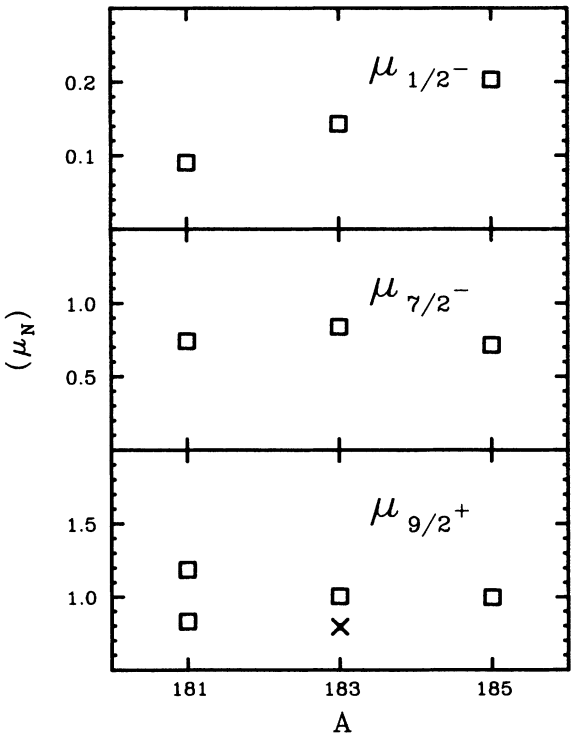

FIG. 14. IBFA-calculated μ values for selected band-head states in the odd-mass Os isotopes (compared with a single experimental point). (The extra lower point for ^{181}Os assumes a $7/2^+$ state.)

The first five terms have been determined from the previous even-even and odd-mass calculations. The last term is the proton-neutron residual interaction, which takes the form,

$$V_{pn} = V_q Q_p \cdot Q_n + V_s \sigma_p \cdot \sigma_n \ . \tag{21}$$

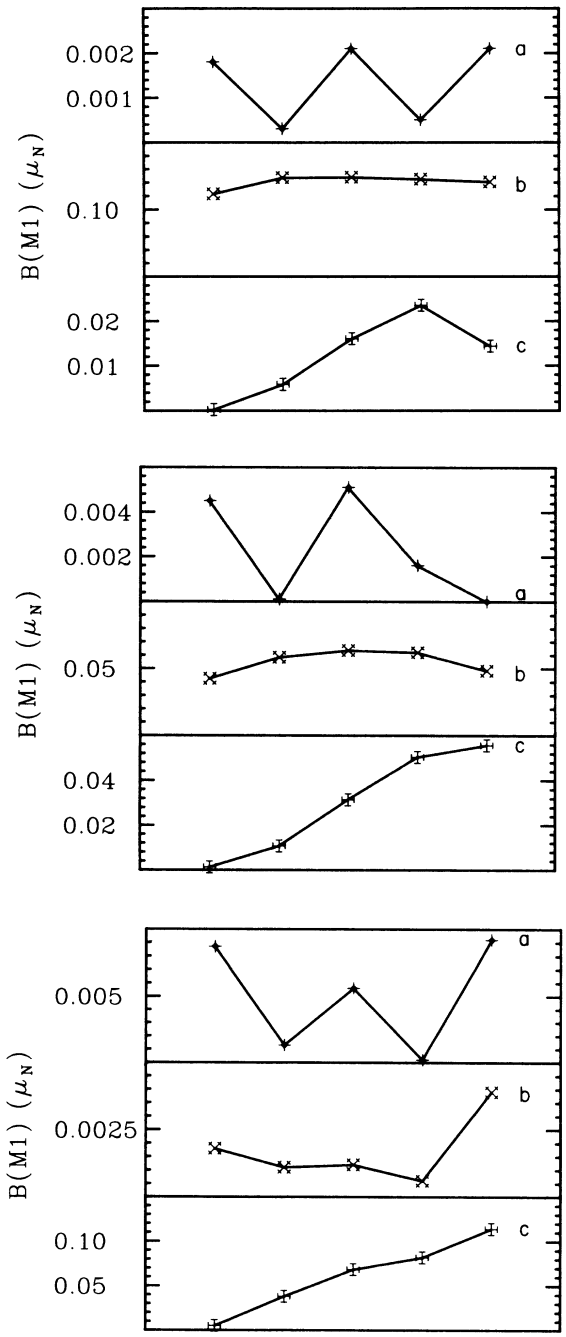

FIG. 15. IBFA-calculated $B(M1)$ values for selected transitions between low-lying rotational-band members in the odd-mass Os isotopes. Top, the values for ^{181}Os; middle, for ^{183}Os; bottom, for ^{185}Os. Within each figure the curves show transitions within bands as follows: *a*, $1/2^-$ band; *b*, $7/2^-$; and *c*, $9/2^+$. Transitions between the lowest members of a band lie on the left, between members increasing systematically toward the right, as in Fig. 6.

The structure of these nuclei is dominated by the features of each of the odd particles that are coupled to the core. The proton-neutron residual interaction plays a relatively minor role because its dominant component is a quadrupole-quadrupole force. Most of the quadrupole corrections have already been included in the particle-boson interaction. The effect of the residual interaction to enhance these correlations is thus small. This is confirmed by numerical calculations. Therefore, we neglected the residual even multipole interaction between the proton and neutron.

The above arguments, however, are not valid for the odd-tensor components. Of special interest is the proton-neutron spin-spin interaction, the last term in Eq. (21). The expectation value of σ for bosons is small, because of their large quadrupole collectivity. In addition, expectation values of odd-rank tensors are not enhanced by collectivity in the boson space, contrary to what happens for even-rank tensors. Since this interaction is not taken into account in the particle-boson interactions, we retain it in the residual interaction. Its effect is well known, introducing a triplet-singlet splitting of the order of 100 keV or less.

In order to make numerical calculations feasible, we have truncated the full two-quasiparticle basis space. In the calculation of ^{182}Re, for example, we first calculated ^{183}Os in the full basis of one neutron in all possible orbits coupled to the complete core. From this calculation we retained only the 15 lowest eigenstates for each spin. To these states the degrees of freedom of the odd-proton hole were coupled. The Hamiltonian was then diagonalized in this truncated space. The advantage of this truncation procedure is that it can also be done in reverse order, i.e., first couple the proton to the even-even core, diagonalize, truncate, and then finally couple the odd neutron. By comparing the results of the two calculations, a good estimate can be obtained of the effects of the basis-space truncation. We have verified that for the present calculation this change of the coupling order reproduces the energies of the levels of interest to within 20 keV. In addition, transition rates, which will be discussed in the next section, were reproduced accurately. As a last check we verified that decreasing the number of levels of the odd-mass intermediate-coupling basis from 15 to 12 for each spin changed the energies of interest by less than 10 keV.

In our calculations we chose the strength of V_s to be -0.02 MeV, constant for all orbits and isotopes. This reproduces reasonably well the triplet-singlet splitting observed near closed shells. The calculated energy spectra are shown in Figs. 16–18, where they are compared with the available experimental data.[20–24]

Experimental data are most complete for ^{182}Re (Ref. 20), where four rotational bands plus a few other states have been characterized in considerable detail. The 7^+ ground state and the 2^+ state are the triplet and singlet couplings of the $\pi 5/2^+[402\uparrow]$ (originating from the $d_{5/2}$ spherical state) and the $\nu 9/2^+[624\uparrow]$ (from the $i_{13/2}$ spherical state) orbits. Because of the excessively long half-life for an $M5$ γ-transition between these states, each decays independently by β^+/ϵ and the energy splitting is unknown. Our calculations predict the 2^+ state to lie at

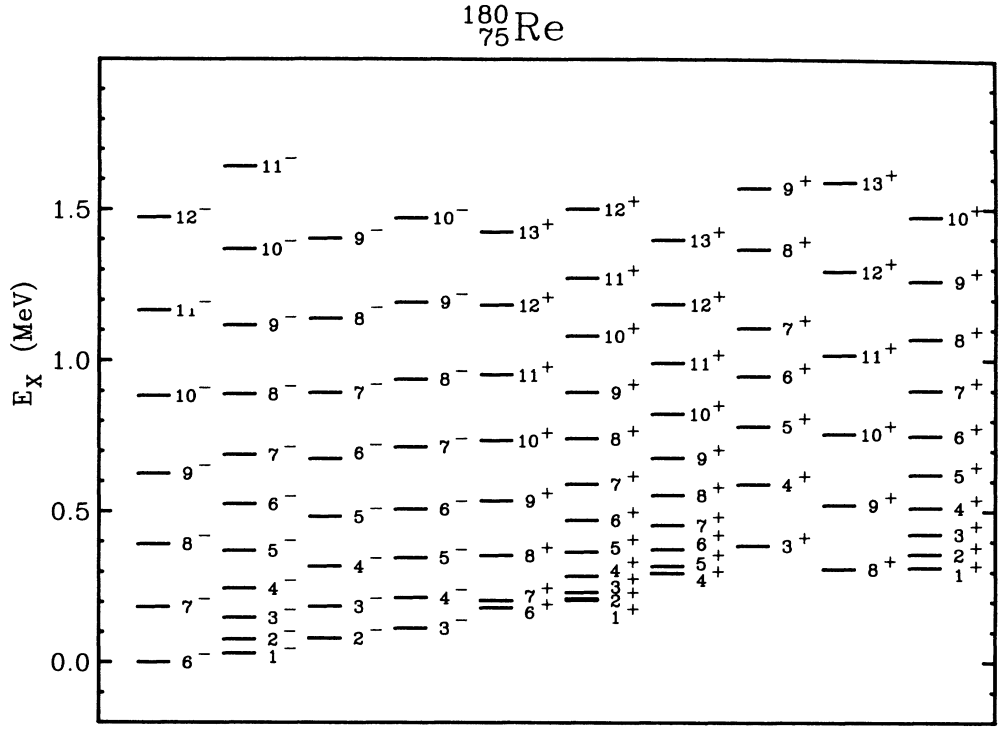

FIG. 16. IBFFA-calculated excitation energies for states in odd-odd ^{180}Re. The bands come in pairs, with the triplet coupling on the left and the singlet coupling on the right. For example, the 6^- band is the triplet coupling, the 1^- band the singlet coupling of a $5/2^+$ proton with a $7/2^-$ neutron state.

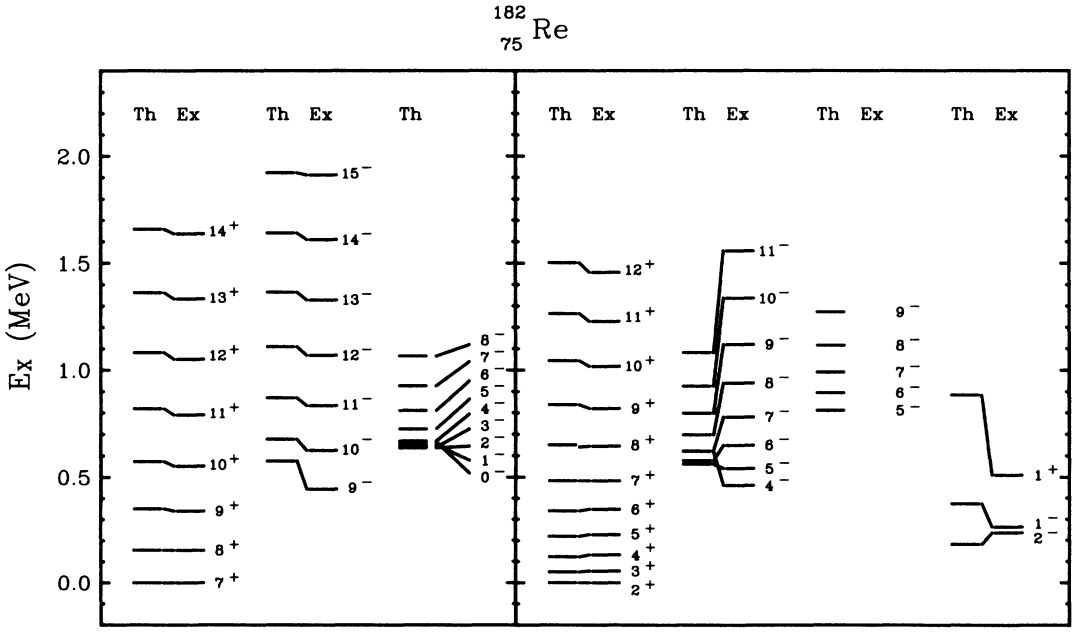

FIG. 17. IBFFA-calculated excitation energies for states in odd-odd ^{182}Re compared with experimental data. Because the experimental separation between the 7^+ triplet and 2^+ singlet couplings is not known, the figure is divided into two parts, using each coupling as the reference point. Otherwise, the triplet coupling is shown on the left of a pair of bands, the singlet coupling on the right. For example; 9^- triplet, 0^- singlet.

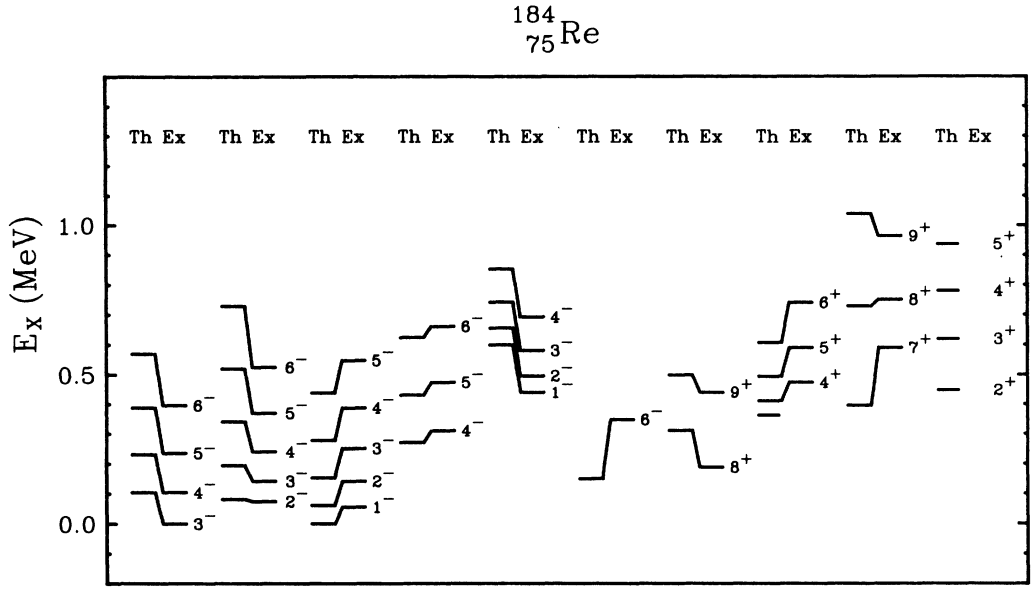

FIG. 18. IBFFA-calculated excitation energies for states in odd-odd ^{184}Re compared with experimental data. The bands are plotted in pairs, with the triplet coupling on the left, the singlet coupling on the right of each pair.

38.6 keV, but we plot the two halves of the energy spectrum in Fig. 17 separately, one with 7^+, the other with 2^+ as the base. The results agree well with experimental data, except for the 4^- band. The reason for this discrepancy lies in the fact that in the calculation there is a close-lying 5^- band. Because of the coriolis force, which is *not* attenuated in the present calculations, these two bands mix strongly, with the result that the lowest member of the $K^\pi=4^-$ band is a 5^- state. We obtain quite reasonable values for the triplet-singlet splittings for the bands shown, although this is not always true for some higher-lying bands.

Although at least six rotational bands have been observed[22,23] in ^{180}Re, assignments are considerably less certain for this nucleus. In fact, our calculations are incompatible with the first tentative assignments made to some of the bands on the basis of $M1/E2$ mixing ratios.[22] For this reason, in Fig. 16 we show only the results from our calculations, which predict a wealth of relatively low-lying, low-spin bands. More meaningful comparisons with experiment must await a more detailed analysis of the experimental data, but we shall discuss this further in Sec. V.

A number of rotational bands have been observed in ^{184}Re, but only the ground-state 3^- and an 8^+ band having its band head at 188 keV have been given definite assignments.[22] We show a comparison of our results with these data in Fig. 18. Our calculations indicate the two bands mentioned above, plus tentatively-assigned 1^- and 2^- bands starting at 56 and 74 keV, respectively. The spacings within the bands is reproduced quite well, but there are minor problems with the positions of the band heads themselves. In particular, note that we calculate the 2^- band head to lie below the 3^- band head when the reverse is observed. The most probable interpretation for these states is that they are the triplet and singlet couplings of a $\pi 5/2^+[402\uparrow]$ and a $\nu 1/2^-[510\uparrow]$ Nilsson state, so the singlet would appear to lie lower in energy than the triplet. However, there is considerable mixing of the $1/2^-$ neutron states in the odd-mass Os isotopes, and our calculations would indicate large contributions from $1/2^-[521\downarrow]$ and $1/2^-[501\downarrow]$ states, so the question of triplet versus singlet couplings becomes a bit obscure.

B. Quadrupole properties

Quadrupole transitions in medium-heavy nuclei are in general of the order of several hundreds of single-particle units. In the calculation of strong, collective transitions, therefore, the contributions from the odd proton and odd neutron are unimportant. We thus limited the $E2$ transitions operator to that defined in Eq. (4), with the boson effective charge e_B the same as enters into the description of $E2$ properties in the even-even core and the two related odd-mass nuclei. Some selected $B(E2)$ values are shown in Fig. 19, and we list various Q values in Table VIII. It can be seen that these are rather generalized (collective) properties that depend little on the specific fermion combinations. Agreement with experimental values[20–24,49,50] looks reasonable.

TABLE VIII. Quadrupole moments for odd-odd Re isotopes.

Isotope	J^π	$Q_{\rm IBA}$ (e b)	$Q_{\rm exp}$ (e b)
^{180}Re	6^-	6.50	
	1^-	6.45	
^{182}Re	7^+	5.66	<6.4
	2^+	5.40	>6.6
^{184}Re	3^-	5.06	7.9 ± 0.7
	8^+	4.83	

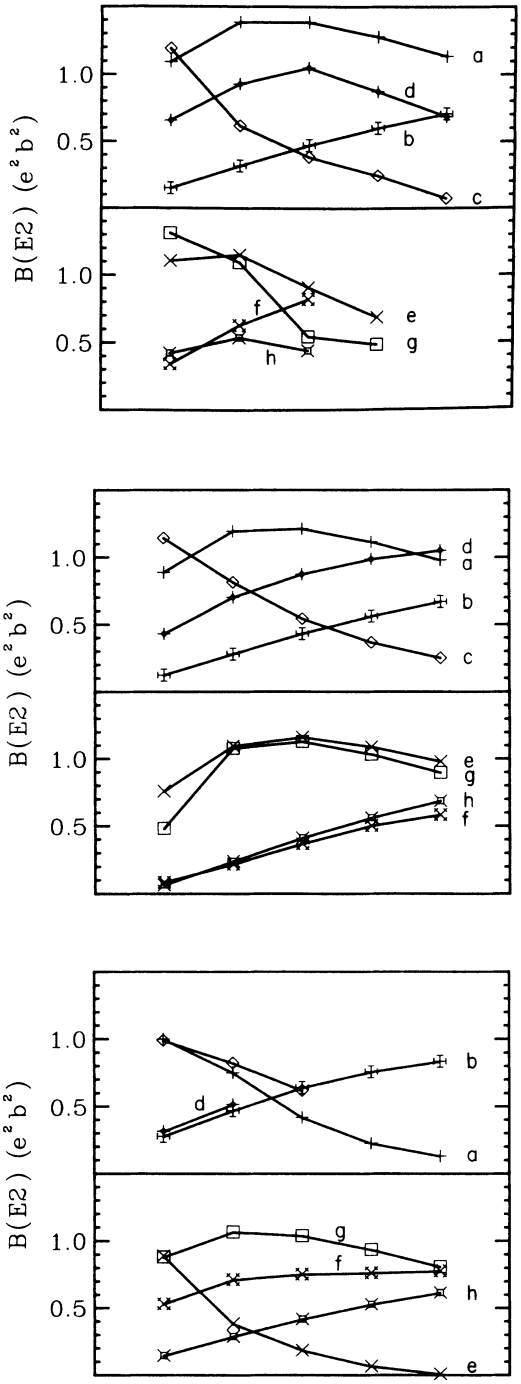

FIG. 19. IBFFA-calculated $B(E2)$ values for selected crossover and stopover transitions between members of low-lying bands in the odd-odd Re isotopes. Top, values for ^{180}Re; the curves correspond to transitions in bands as follows: *a*, 6^- stopover; *b*, 6^- crossover; *c*, 1^- stopover; *d*, 1^- crossover; *e*, 2^- stopover; *f*, 2^- crossover; *g*, 3^- stopover; and *h*, 3^- crossover. Transitions between the lowest members of a band lie at the left, with transitions between systematically increasing members more toward the right, as in Fig. 6. Middle, values for ^{182}Re; *a*, 7^+ stopover; *b*, 7^+ crossover; *c*, 2^+ stopover; *d*, 2^+ crossover; *e*, 9^- stopover; *f*, 9^- crossover; *g*, 4^- stopover; and *h*, 4^- crossover. Bottom, values for ^{184}Re; *a*, 3^- stopover; *b*, 3^- crossover; *c*, 2^- stopover; *d*, 2^- crossover; *e*, 1^+ stopover; *f*, 1^+ crossover; *g*, 8^+ stopover; and *h*, 8^+ crossover.

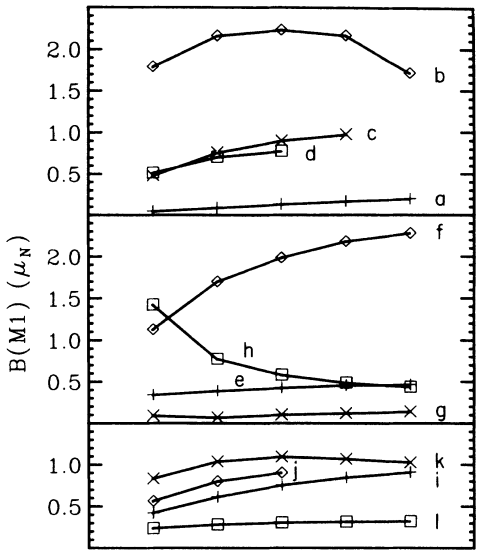

FIG. 20. IBFFA-calculated $B(M1)$ values for selected transitions among low-lying band members in the odd-odd Re isotopes. The curves represent transitions in bands as follows. ^{180}Re: *a*, 6^-; *b*, 1^-; *c*, 2^-; and *d*, 3^-. ^{182}Re: *e*, 7^+; *f*, 2^+; *g*, 9^-; and *h*, 4^-. ^{184}Re: *i*, 3^-; *j*, 2^-; *k*, 1^-; and 1, 8^+. Transitions between the lowest members of bands lie at the left, with transitions between systematically increasing members toward the right, as in Fig. 6.

C. Magnetic dipole properties

Contrary to quadrupole transitions, $M1$ transitions are at most of the order of a few single-particle units. The single-particle part of the operator, as given in Eq. (18), thus plays the same important role it did in the odd-mass calculations. Our calculation procedures were similar to those used for the odd-mass nuclei, with the *d*-boson *g* factor equal to the *g* factor for the 2_1^+ states in the even-even core, g_s quenched by a factor of 0.7, and g_l taken equal to their free values. Note that in even-even nuclei the first term of Eq. (18) does not induce $M1$ transitions, since it is proportional to the total angular-momentum operator. In odd-odd nuclei, however, just as in odd-mass nuclei, all terms can contribute to both the magnetic moments and $M1$ transition rates.

Some calculated $B(M1)$ values are shown in Fig. 20, and some μ values are listed in Table IX. It can be seen that they are determined primarily by the fermion portion of the operator. Relatively few experimental data

TABLE IX. Magnetic moments for odd-odd Re isotopes.

Isotope	J^π	$\mu_{\rm IBA}(\mu_N)$	$\mu_{\rm exp}(\mu_N)$
^{180}Re	6^-	2.41	
	1^-	2.35	
^{182}Re	7^+	2.33	2.76±0.07
	2^+	3.28	3.07±0.24
^{184}Re	3^-	3.19	2.50±0.19
	8^+	2.09	2.89±0.13

TABLE X. Comparison of IBA and Bohr-Mottelson predictions for ^{182}Re.

J^π (triplet) J^π (singlet)	Exp. E_x (keV)	IBA E_x (keV)	BM E_x (keV)	Nilsson states Proton	Neutron
7^+	0	0	0[a]	$5/2^+[402\uparrow]$	$9/2^+[624\uparrow]$
2^+	Δ[b]	38.6	δ[a]		
9^-	443.1	575.5	259.6	$9/2^-[514\uparrow]$	$9/2^+[624\uparrow]$
0^-		664.3	δ		
4^-	$\Delta+461.3$[b]	621.1	599.0	$1/2^-[541\downarrow]$	$9/2^+[624\uparrow]$
5^-		811.6	δ		

[a]We made no attempt to calculate the triplet-singlet splitting in the Bohr-Mottelson formalism; hence, E_x (triplet) is really the center of gravity for the two states, and δ is the unknown triplet-singlet splitting.
[b]The experimental triplet-singlet splitting Δ is not known.

exist for comparison, but one notable result occurs in ^{182}Re, where it can be seen that the $B(M1)$ values, hence the stopover transitions, are larger for the 2^- singlet coupling than for the 7^- triplet coupling of the $\pi 5/2^+[402\uparrow]$ and $\nu 9/2^-[624\uparrow]$ states.

V. CONCLUSIONS AND COMPARISONS

The IBFFA model is able to give an accurate description of states in the odd-odd Re nuclei, as can be seen from the comparisons with experimental data in Figs. 17 and 18. These odd-odd nuclei constitute a very stringent test of the model, because odd-odd nuclei do not provide the same sort of smoothly varying systematics as do other types of nuclei. Also, errors tend to accumulate: Any difficulties in describing the even-even cores and, particularly, the odd-mass states are compounded in the odd-odd systems. However, if good fits for the even cores and for the odd-mass states can be obtained, then good spacings in the odd-odd nuclei are likely. This can be seen in our calculations, where the poorest fits obtained for odd-mass states were for the $1/2^-$ bands in the odd-mass Os isotopes. Correspondingly, relatively poor fits were obtained for odd-odd bands involving these $1/2^-$ neutrons, such as inverting the triplet and singlet couplings for the 3^- and 2^- bands in ^{184}Re. Also, in ^{182}Re the 4^- band, which involves a $1/2^-$ proton, had the poorest fit. (Of course, adequate fits to $J=1/2$ bands are an inherent problem in any description, not just limited to an IBFA model.) In general, we obtained good fits for spacings within the bands but had some problems with the positions of the band heads and with the triplet-singlet coupling spacings. This points to difficulties in V_{pn}, the proton-neutron residual interaction. (Again, this is recognized as a decades-old problem with calculations involving odd-odd nuclei.) A simple first-stage improvement would be to free V_q and especially V_s, allowing them to vary over a reasonable range. In addition, it should be remembered that in the present calculations we did not need to introduce an attenuation in the coriolis force.

In order to shed a different light on the results of our calculations, we have made a comparison with the results of some simple, Nilsson-like calculations.

A major difference between an IBA calculation and the Bohr-Mottelson (BM) model lies in the definition of the bases. In the BM model all calculations are performed in the intrinsic system, using deformed basis states. For this reason, for example, the coriolis force appears explicitly

TABLE XI. Comparison of IBA and Bohr-Mottelson predictions for ^{180}Re.

J^π (triplet) J^π (singlet)	IBA E_x (keV)	BM E_x (keV)	Nilsson states Proton	Neutron
1^-	30.1	0[a]	$5/2^+[402\uparrow]$	$7/2^-[514\downarrow]$
6^-	0	δ[a]		
2^-	80.6	Δ[b]	$5/2^+[402\uparrow]$	$1/2^-[521\downarrow]$[b]
3^-	113.6	δ		
6^+	181.5	?[b]	$5/2^+[402\uparrow]$	$7/2^+[633\uparrow]/9/2^+[624\uparrow]$[b]
1^+	212.1	δ		
4^+	297.3	356.7[c]	$1/2^-[541\downarrow]$[c]	$7/2^-[514\downarrow]$
3^+	387.0	δ		

[a]δ is the unknown triplet-singlet splitting; cf. Table X.
[b]These two neutron states form a "mixed" $i_{13/2}$ band, making it difficult to predict the bandhead E_x within the BM framework.
[c]From the $h_{9/2}$ spherical orbit, this state has an enormous decoupling parameter, making an odd-odd E_x estimate difficult.

TABLE XII. Comparison of IBA and Bohr-Mottelson predictions for ^{184}Re.

J^π (triplet) J^π (singlet)	Exp. E_x (keV)	IBA E_x (keV)	BM E_x (keV)	Nilsson states Proton	Neutron
3^-	0	104.1	0[a]	$5/2^+[402\uparrow]$	$1/2^-[510\uparrow]$
2^-	74	81.4	δ[a]		
1^-	56	0	23.5	$5/2^+[402\uparrow]$	$3/2^-[512\downarrow]$
5^-		271.5	δ		
8^+	188.01	311.2	197.4	$5/2^+[402\uparrow]$	$11/2^+[615\uparrow]$
3^+		362.4	δ		

[a]δ is the unknown triplet-singlet splitting; cf. Table X.

in the Hamiltonian. In the IBA model all calculations are performed in the laboratory system, so the coriolis force is "hidden" in the Hamiltonian. It is automatically included because the core has a finite moment of inertia. Another difference arises from the fact that the IBA model is formulated in a spherical basis. The residual interaction between the odd particles can thus be linked directly to the residual interaction in the usual spherical shell model.

We begin with ^{182}Re, which has the best-understood experimental data, with definite Nilsson states assigned to each band.[20] We used a semiempirical, almost simplistic method for predicting the excitation energies of the odd-odd states, taking the sums of the appropriate single-particle energies from the odd-mass neighbors. In a sense this is an unfair use of the Bohr-Mottelson model, yet in another sense it is giving it the benefit of the doubt, for experimental energies (known to be accurate) are used rather than calculated Nilsson-state energies, which would involve many more unknown parameters. Hoff and his collaborators[51,52] have calculated odd-odd nuclear states for actinide nuclei, using a semiphenomenological Bohr-Mottelson treatment, and they have obtained rather successful results. We have also used their approach, calculating states in ^{250}Bk.[53] However, in the present paper for simplicity we retain the simpler application of the Bohr-Mottelson model.

In Table X we present a qualitative comparison of the excitation energies of the band heads as determined by the two models. Also, no attempt was made to calculate the triplet-singlet energy splittings, so the energy listed for the triplet states is in actuality something like a center of gravity for the triplet-singlet pair of states. It can be seen that predictions from both models are adequate, although the IBA model yields more detailed predictions. (Again, this is not a completely fair assessment of the Bohr-Mottelson model, and a more detailed calculation in that framework could improve the comparison. However, that would involve a major research effort in itself, and it is certainly beyond the scope of this paper.)

In Table XI we show a comparison between the predictions of the two models for ^{180}Re. The only experimental assignment we can trust for this nuclide is the 1^- ground state, which is correctly predicted by the Bohr-Mottelson formalism as the triplet coupling of the $\pi 5/2^+[402\uparrow]$ and $\nu 7/2^-[514\downarrow]$ states. Here the IBA model predicts the 6^- singlet coupling of these same states to lie some 30 keV lower. Both models predict a number of low-spin states, including $K=3$ and 4 states. (Certain such states were very tentatively assigned[23] to some bands in ^{180}Re, but these assignments are not consistent with the predictions of either model; among other problems, the spacings between band members is unreasonably large for such low-K values. See Ref. 19 for a discussion of how this might be explained by coriolis mixing in higher-K bands.) Thus, at this time an experiment cannot distinguish very well between the two models. What Table XI does point out, however, is that for certain problem cases, such as the "mixed" $i_{13/2}$ band and for the $1/2^-[521\downarrow]$ neutron state with an abnormally large decoupling parameter (i.e., very large coriolis matrix elements), predictions are easier to make via the IBA formalism. And remember that the positions of band heads have been the weakest point in our calculations—spacings within the bands come out much better, even when they involve large coriolis-induced distortions.

Finally, in Table XII we present the comparison for ^{184}Re. Predictions from both models are again reasonably acceptable, although our IBA calculations invert the triplet and singlet members of the lowest coupling, as discussed above.

In conclusion, IBFFA calculations of state energies and electromagnetic properties for deformed odd-odd nuclei work rather well. The calculations predict (and reproduce) band spacings, including distortions, quite well; band-head energies show larger deviations from experimental values. They also yield reasonable quantitative agreement with the electromagnetic properties, although relatively few data are currently available for checking these. More extensive calculations, including calculations for more extended series of isotopes should provide a more stringent test of the model. They may also help us to develop a better understanding of the physical correspondences to the IBA group-theoretical parameters.

ACKNOWLEDGMENTS

We thank Dr. R. Aryaeinejad and Mr. Wade Olivier for help in carrying out the calculations. This work was supported by the U.S. National Science Foundation under Grant No. PHY-85-19653.

[1]A. Arima and F. Iachello, Phys. Rev. C **14**, 761 (1976).
[2]A. Arima and F. Iachello, Ann. Phys. (N.Y.) **99**, 253 (1976).
[3]A. Arima and F. Iachello, Ann. Phys. (N.Y.) **111**, 201 (1979).
[4]A. Arima and F. Iachello, Ann. Phys. (N.Y.) **123**, 468 (1979).
[5]O. Scholten, F. Iachello, and A. Arima, Ann. Phys. (N.Y.) **115**, 325 (1979).
[6]R. F. Casten and J. A. Cizewski, Nucl. Phys. **A309**, 477 (1978).
[7]I. Talmi, in *Short-Distance Phenomena in Nuclear Physics,* edited by D. H. Boal and R. H. Woloshyn (Plenum, New York, 1983), p. 311.
[8]F. Iachello and O. Scholten, Phys. Rev. Lett. **43**, 679 (1979).
[9]O. Scholten, in *Contemporary Research Topics in Nuclear Physics,* edited by D. H. Feng, M. Vallieres, M. W. Guidry, and L. L. Riedinger (Plenum, New York, 1985), p. 503.
[10]O. Scholten and N. Blasi, Nucl. Phys. **A380**, 509 (1982).
[11]A. B. Balantekin, I. Bars, and F. Iachello, Phys. Rev. C **47**, 19 (1981).
[12]T. Hubsch and V. Paar, Z. Phys. A **319**, 111 (1984).
[13]V. Paar, Proceedings of International Symposium on Capture Gamma-Rays, Leuven, 1987 (unpublished).
[14]N. Blasi (private communication).
[15]S. Brandt, V. Paar, and D. Vretenar, Z. Phys. A **319**, 355 (1984).
[16]V. Lopac, S. Brandt, V. Paar, O. W. B. Schult, H. Seyfarth, and A. B. Balantekin, Z. Phys. A **323**, 491 (1986).
[17]A. B. Balantekin, I. Bars, and F. Iachello, Phys. Rev. C **47**, 19 (1981).
[18]A. Gelberg and A. Zemel, Phys. Rev. C **22**, 937 (1980).
[19]A. Faessler, Nucl. Phys. **A396**, 291c (1983).
[20]M. F. Slaughter, R. A. Warner, T. L. Khoo, W. H. Kelly, and Wm. C. McHarris, Phys. Rev. C **29**, 114 (1984).
[21]Wm. C. McHarris, W.-T. Chou, J. Kupstas-Guido, and W. Olivier, in *Nuclei Off the Line of Stability,* Symposium Series No. 324 (American Chemical Society, Washington, D.C., 1986), p. 329.
[22]R. M. Lieder, Proceedings of the XXIII International Winter Meeting on Nuclear Physics, Bormio, Italy, 1985, p. 276.
[23]Ts. Venkova, R. M. Lieder, T. Morek, W. Gast, G. Hebbinghaus, A. Krämer-Flecken, J. Schäffler-Kräh, W. Urban, H. Kluge, K. H. Maier, A. Maj, and G. Sletten, KFA Jülich, Annual Report for 1985.
[24]M. J. Martin and P. H. Stelson, Nucl. Data Sheets **21**, 1 (1977).
[25]See, e.g., A. Bohr and B. R. Mottelson, *Nuclear Structure* (Benjamin, Reading, Mass., 1975), Vol. II, and references therein.
[26]O. Scholten, Ph.D. thesis, University of Groningen, 1980.
[27]C. Faklander and G. D. Dracoulis, Nucl. Phys. **A375**, 263 (1982).
[28]R. Hochel, P. J. Daly, and K. J. Hofstetter, Nucl. Phys. **A211**, 165 (1973).
[29]M. R. Schmorak, Nucl. Data Sheets **13**, 267 (1974).
[30]M. V. Hoehn, E. B. Shera, Y. Yamazaki, and R. M. Steffen, Phys. Rev. Lett. **39**, 1313 (1977).
[31]S. A. Lane and J. X. Saladin, Phys. Rev. C **6**, 613 (1972).
[32]R. Levy, N. Tsoupas, N. K. B. Shu, A. Lopez-Garcia, W. Andrejtscheff, and N. Benczer-Koller, Phys. Rev. C **25**, 293 (1982).
[33]O. Scholten and A. E. L. Dieperink, in *Interacting Bose-Fermi Systems in Nuclei,* edited by F. Iachello (Plenum, New York, 1981), p. 343.
[34]P. P. Singh, L. D. Medsker, G. T. Emery, L. A. Beach, and C. R. Gossett, Phys. Rev. C **10**, 656 (1974).
[35]A. Neskakis, R. M. Lieder, M. Müller-Veggian, H. Beuscher, W. E. Davidson, and C. Mayer-Böricke, Nucl. Phys. **A261**, 189 (1976).
[36]R. B. Firestone, Nucl. Data Sheets **43**, 289 (1984).
[37]A. Artna-Cohen, Nucl. Data Sheets **16**, 267 (1975).
[38]Y. A. Ellis-Akovali, Nucl. Data Sheets **33**, 557 (1981).
[39]E. Hagn and E. G. Eska, Nucl. Phys. **A363**, 269 (1981).
[40]H. Ernst, E. Hagn, and E. Zech, Phys. Rev. C **23**, 1739 (1981).
[41]R. Spanhoff, M. J. Canty, H. Postma, and G. Mennenga, Phys. Rev. C **21**, 361 (1980).
[42]S. Büttgenbach, R. Dicke, G. Gölz, and F. Träber, Z. Phys. A **302**, 281 (1981).
[43]K. M. Bisgård and E. Veje, Nucl. Phys. **A103**, 51 (1967).
[44]F. M. Bernthal, J. S. Boyno, C. L. Dors, T. L. Khoo, and R. A. Warner, MSU Cyclotron Laboratory Annual Report for 1972-73, p. 72; C. L. Dors, F. M. Bernthal, and R. A. Warner, *ibid.,* p. 74.
[45]I. M. Ladenbauer-Bellis, H. Bakhru, and P. Sen, Nucl. Phys. **A252**, 524 (1975).
[46]I. M. Landenbauer-Bellis, P. Sen, and H. Bakhru, Can. J. Phys. **56**, 321 (1978).
[47]E. Hagn and E. Zech, Z. Phys. A **295**, 345 (1980).
[48]Th. Lindblad, R. Bethoux, R. H. Price, and P. Kleinheinz, Nucl. Phys. **A217**, 459 (1973).
[49]K. S. Krane, C. E. Olsen, and W. A. Steyert, Phys. Rev. C **7**, 263 (1973).
[50]H. Hübel and C. Günther, Nucl. Phys. **A210**, 317 (1973).
[51]T. von Egidy, R. W. Hoff, R. Lougheed, D. H. White, H. G. Börner, K. Schreckenbach, D. D. Warner, and P. Hungerford, Phys. Rev. C **29**, 1243 (1984).
[52]R. W. Hoff, J. Kern, R. Piepenbring, and J. P. Boisson, in *Capture Gamma-Ray Spectroscopy and Related Topics-1984,* Proceedings of the International Symposium, Knoxville, Tennessee, edited by S. Raman (AIP Conf. Proc. No. 125) (AIP, New York, 1985), p. 274.
[53]I. Ahmad, Z. M. Koenig, and Wm. C. McHarris (unpublished).